A New Bio Inspired Majority Device MAJ (A, B, C)

Ommolbanin Moghimi Kandelous [a] *, Norassadat Moosavi [b], Mahya Sam Daliri [c], Keivan Navi [d]

[a] *Khatam University, Tehran, Iran*
[b] *Islamic Azad University Central Tehran Branch, Tehran, Iran*
[c] *Faculty of Computer Science and Engineering, Shahid Beheshti University, Tehran, Iran*
[d] *Faculty of Computer Science and Engineering, Shahid Beheshti University, Tehran, Iran*

Abstract
In this article, we try to model the effect of the changes of the threshold voltage of two positive inputs to negative ones using nanotechnology-based on Quantum Dot Cellular automata (QCA). In order to do so, the voter of a Majority cell has been modified resulting in amplifying the negative effect of the upper and the lower cells. Besides this Brain-inspired approach can be used to design a very fast Majority function with two negative inputs based on QCA.

Keywords: Neural Network, Bio-inspired nanostructure design, Nanotechnology, QCA, Power consumption, Majority Gate.

1. Introduction

One of the most atractive approaches in order to design nano structure circuit is to be inspired from the nature and namely Bio inspired techniques which are stimulated by the structure and behavior of the human brain. A biological neuron has the potential to help the design of nanoscale circuits and devices. The introduction of the complementary metal-oxide-semiconductors (CMOSs) to digital circuits in the 1960s was a technological revolution which effectively gave birth to the integrated circuit [1]. A well recognized concept in the IC industry is the Moore's law [2], which predicts that the number of transistors on an IC chip doubles nearly every two years. Although the IC technology seems to have followed the

Moore's law prediction in the past few decades, the validity of this prediction in today's and future technology is in doubt.

The CMOS technology suffers from fundamental limitations, including the need for a high number of minimum fabrication dimensions as well as the off-state leakage. Such limitations are even more serious in the sub 20 nm dimensions [3]. In this study, we discuss the quantum dot cellular automata(QCA) devices as a supplemental or even a potential alternative to the CMOS technology.

The QCA devices were first introduced by Lent in 1993 [4]. Amongst others, small dimensions (nm), ultra-low power consumption, and high clock rates are the crucial advantages of the QCA that place this technology in a strong position as a potentially suitable alternative to CMOS [5]. Since the future of circuit technology is moving towards further size-miniaturization, commercializing the QCA devices could be extremely beneficial to this industrial sector. However, extensive research and budget is needed to achieve this goal, because at present, the QCA circuits are not commercially viable from a production point of view.

In this paper, first the fundamentals of the QCA and Neural Network are reviewed in section 2. Thereafter in section 3, a number of innovative QCA designs in the literature are briefly reviewed. In section 4, we introduced our proposed novel design, with the concluding remarks in section 5.

2.   Background
2.1 QCA Background

The QCA devices are essentially composed of quantum cells with Coulombic interactions. Therefore the building blocks of the QCA technology are the quantum cell. A quantum cell is a square structure, containing four quantum dots located on the four corners of the square. There are two electrons in each cell. Due to the Coulombic repulsion between the electrons, only two stable electronic states exist inside each cell. These stable states are located on the diagonals of the square, with two distinct polarizations (p= -1 and p=+1), forming the binary functions [6], [7].

Electrons can move between the dots through quantum tunneling events. In the QCA devices, power is consumed in the cells when a clocking scheme takes place. As the barriers are raised, a considerable amount of energy is transferred to the cell. The interdot tunneling energy is 0.3 meV. The width of each cell is 18 nm and the distance between the neighboring cells is 2 nm. Fig 1 is a schematic of these cells.
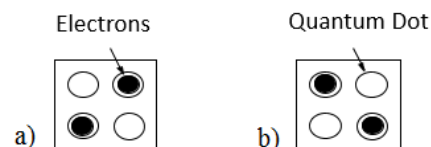

Fig. 1 Scheme of the basic cell a) P=+1 (logic1). b) P=-1 (logic 0).

A linear array of cells creates a QCA wire. There are two types of QCA wires: normal wires and rotate wires [8]. All QCA circuits consist of a combination of gates and wires. Thus, gate behavior plays an

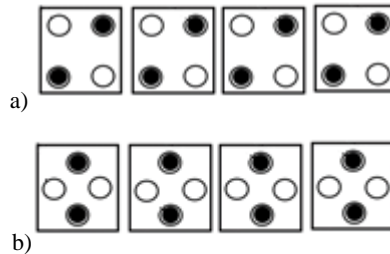important role in the QCA technology [9]. (See Fig 2)

a)

b)

Fig. 2 Scheme of the wire a) Normal wire. b) Rotate wire.

The basic gate in QCA is the majority gate (MAJ)[10]. A majority gate is a voter circuit, which votes to majority inputs. Inputs are always odd numbers and greater than one[11]. The AND gate and the OR gate are designed with the MAJ. The MAJ has three inputs, as described in equation (1).

M (A, B, C) = AB+BC+AC   (1)

The simplest majority gate includes five cells. Three of them are input cells. The other two cells are voter and output cells [2]. In Fig 3, one three-input majority gate has been illustrated, and its truth table is presented in Table 1.
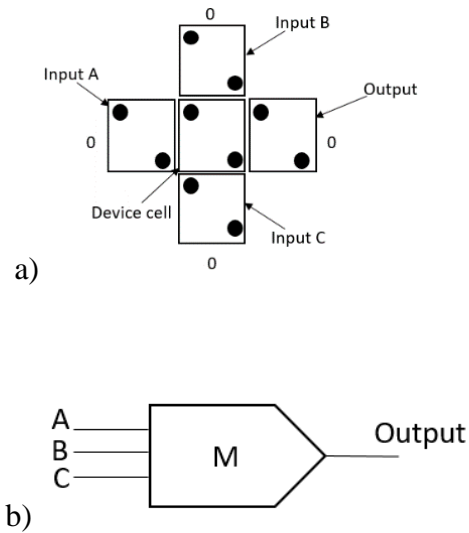

a)

b)

Fig. 3 Cell level. (a) The Scheme. (b)

Table 1 The truth table of three-input Majority Function

A	B	C	Out
0	0	0	0
0	0	1	0
0	1	0	0
0	1	1	1
1	0	0	0
1	0	1	1
1	1	0	1
1	1	1	1

2.2 Neural Network Background

Artificial Neural Network is inspired from Natural Neural network. Many logic and arithmetic designs are based these natural networks as mentioned in [12], [13], [14]. In Principe the logic design of neural networks are based on defining the required threshold voltage as well as the number of inputs and their related weights. A neurone takes a different set of weighted inputs, applies a summation function of them. Once the summation reaches a threshold, the neuron fires. Beside one can use the configuration of connecting these systems to each other to represent an arithmetic and logic operation. Table 2 illustrates the realization of AND, OR, Majority function and 3-input XOR gates.

Table 2 The truth table of logical gates

A B C	AND TD=2.5	OR TD=0.5	MAJ TD=1.5	XOR= MAJ(A,B,C, 2MIN(A,B,C)
0 0 0	0	0	0	0
0 0 1	0	1	0	1
0 1 0	0	1	0	1
0 1 1	0	1	1	0
1 0 0	0	1	0	1
1 0 1	0	1	1	0
1 1 0	0	1	1	0
1 1 1	1	1	1	1

As seen in table2 the AND gate is realized with the addition of 3 inputs A, B and C as well as defining the required threshold to 2.5. The reason of choosing 2.5 as the threshold voltage is that we consider the possible noise. In the very same way the OR gate is designed with threshold equal to 0.5. When 2 or 3 inputs are equal to logical 1 then the output of MAJ (MAJORITY) gate is equal to logical 1. That is why we choose the related threshold to be 1.5. The most attractive one is the XOR gate witch is implemented in two phases. First, the Majority of inputs is obtained then a five input MAJORITY gate is used as illustrated in table2. MINORITY (MIN) function is the inverted output of the MAJ function.

3. State-of-the-art

In 2011, Hook et al. suggested that it is likely that a QCA cell with four dots and two electrons may not be the most efficient and optimal cell [15]. Instead, they proposed a novel cell with two dots and one electron. Several other types of one-electron QCA devices have been proposed, such as a 2:1 multiplexer (Mux) with reversible logic, proposed by Mili Ghosh et al. in 2015 [16]. This is one of the first Mux designs with two dots and one electron. Furthermore, in 2018, Mondal et al. designed a binary semaphore using a two-dimensional QCA cell (two dots and one electron) [17]. They implemented a binary semaphore using J-K flip-flop. In 2019, Farzaneh et al. proposed a novel full adder which switches between three-and five-input periodically [18].

4. Proposed

In this paper, a new Bio-inspired model of a majority gate with a different number of electrons is presented. The proposed design could be implemented in the structure of some types of Full Adders such as [6], [19], [20], [21]

In the proposed design, the voter cell has four dots and one electron, as compared to the four dots and two electrons in the existing designs. Due to this modification in the voter cell, the output will be different from the normal status (with four dots and two electrons). In fact, the left-side cell of the voter cell has a direct effect on it. However, top and bottom cells indirectly affect the voter cell. In Fig 4 all possible situations are illustrated.

A majority gate MAJ (A, $\overline{B}$, $\overline{Cin}$), is implemented with eight cells in default status. However, in this Bio-inspired study, the number of cells is reduced from eight to only five cells. This also means that the number of electrons will be reduced from sixteen to only nine electrons in the proposed idea [Fig 4].
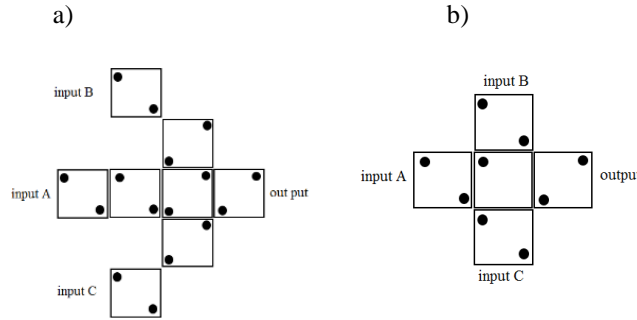
a)   b)

Fig. 4 Majority gate with standard cell (a) majority with proposed device cell. (b)

Equation (2) expresses the coulombic interaction between the cells. In this equation, k is the Coulomb's constant, q_1 and q_2 represent the electrical charge, and r is the distance between two electrons. In this equation, k and q are fixed quantities, so that the numerator remains constant, whilst the denominator varies with distance (Equation (3)).

$$F = \frac{k\,q_1 q_2}{r^2} = \frac{kq^2}{r^2} (q_1 = q_2 = 1.6 * 10^{-19} c), (k \approx 9 * 10^9) \tag{2}$$

$$\frac{kq^2}{r^2} = \frac{9*10^9*(1.6)^2*10^{-38}}{r^2} = \frac{23.04* 10^{-29}}{r^2} = \frac{cte}{r^2} \tag{3}$$

$$F_T = \sqrt{F_1^2 + F_2^2 + 2F_1 F_2 \cos\theta} \tag{4}$$

In order to calculate the cell interactions, the input is set to ABC=000. Based on the results, the cell configuration with minimum cell interaction between the electrons must be chosen so as to achieve a stable state. All possible configurations are shown in Fig.5. The distance between each electron (r) and the electronic charge (q) are substituted into equation (5), in order to calculate the corresponding forces [22], [23]. The forces are divided into F_{T_x} and F_{T_y} . The resultant of these two vectors is F_T, which is calculated by equation (4). When the cell interaction/Coulombic force for each configuration is calculated, the most stable force applied to the charge q needs to be determined. The physical proofs are depicted in the figures (6-9).
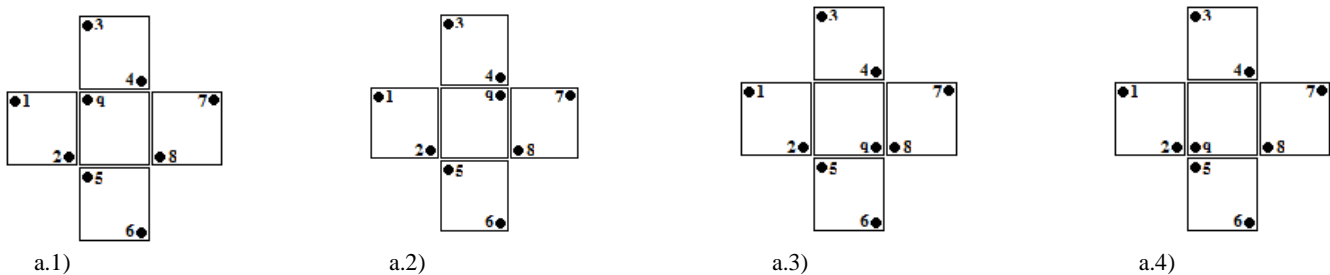

a.1)   a.2)   a.3)   a.4)

Fig. 5 All configurations for the first section whose inputs are ABC=000

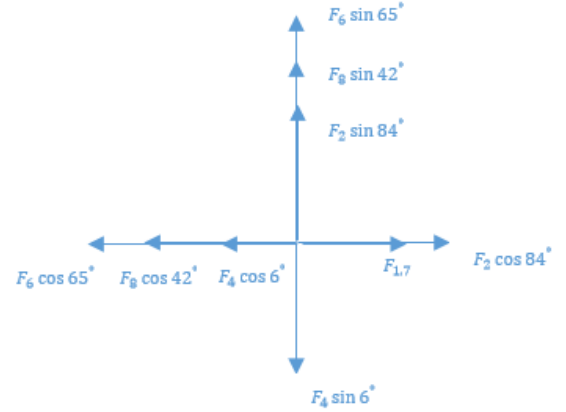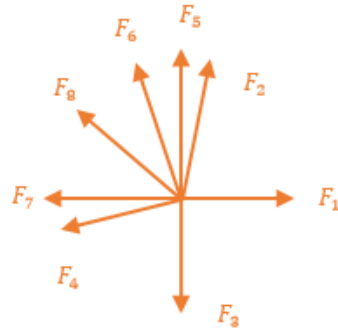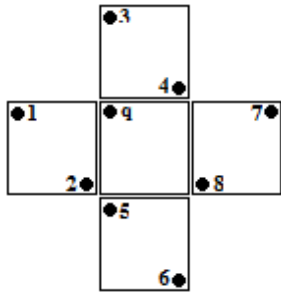**Fig. 6** a.1-1)   a.1-2)   a.1-3)

$$|F_1| = |F_3| = |F_5| = \frac{23.04 * 10^{-29}}{(20*10^{-9})^2} = 0.0576 * 10^{-11}$$

$$|F_2| = |F_4| = \frac{23.04 * 10^{-29}}{328*10^{-18}} = 0.0702 * 10^{-11}$$

$$|F_7| = \frac{23.04 * 10^{-29}}{1444*10^{-18}} = 0.0159 * 10^{-11}$$

$$|F_6| = \frac{23.04 * 10^{-29}}{1768*10^{-18}} = 0.0130 * 10^{-11}$$

$$|F_8| = \frac{23.04 * 10^{-29}}{724*10^{-18}} = 0.0318 * 10^{-11}$$

$$F_{1,7} = F_1 - F_7 = (0.0576 * 10^{-11}) - (0.0159 * 10^{-11}) = 0.0417 * 10^{-11}$$

$$F_{3,5} = F_3 - F_5 = 0$$

$$F_{T_x} = F_4 \cos 6° + F_8 \cos 42° + F_6 \cos 65° - (F_{1,7} + F_2 \cos 84°) = 0.0497 * 10^{-11}$$

$$F_{T_y} = F_2 \sin 84° + F_8 \sin 42° + F_6 \sin 65° - (F_4 \sin 6°) = 0.0951 * 10^{-11}$$

$$\mathbf{F_T = 0.1072 * 10^{-11} \ N}$$

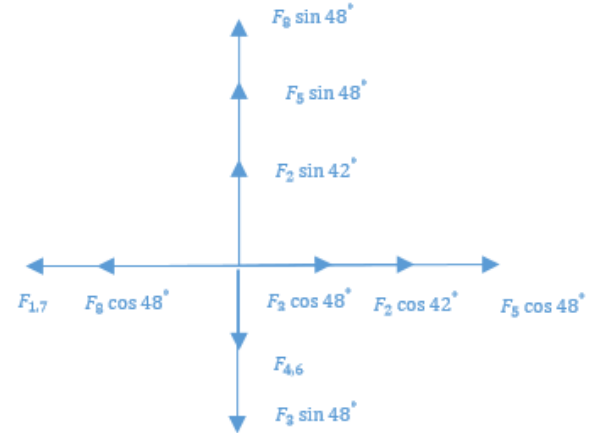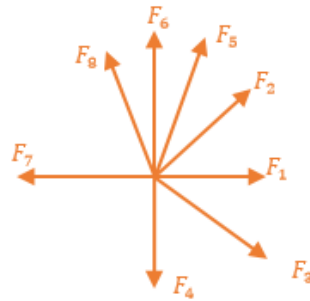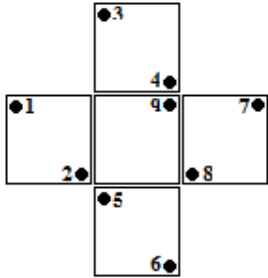**Fig.7** a.2-1)   a.2-2)   a.2-3)

$$|F_1| = |F_6| = \frac{23.04 * 10^{-29}}{(38*10^{-9})^2} = 0.0159 * 10^{-11}$$

$$|F_2| = |F_3| = |F_5| = \frac{23.04 * 10^{-29}}{724*10^{-18}} = 0.0318 * 10^{-11}$$

$$|F_4| = \frac{23.04 * 10^{-29}}{4*10^{-18}} = 5.76 * 10^{-11}$$

$$|F_7| = \frac{23.04 * 10^{-29}}{400*10^{-18}} = 0.0576 * 10^{-11}$$

$$|F_8| = \frac{23.04 * 10^{-29}}{328*10^{-18}} = 0.0702 * 10^{-11}$$

$$F_{1,7} = F_7 - F_1 = (0.0576 * 10^{-11}) - (0.0159 * 10^{-11}) = 0.0417 * 10^{-11}$$

$$F_{4,6} = F_4 - F_6 = (5.76 * 10^{-11}) - (0.0159 * 10^{-11}) = 5.7441 * 10^{-11}$$

$$F_{T_x} = F_{1,7} + F_8 \cos 48° - (F_3 \cos 48° + F_2 \cos 42° + F_5 \cos 48°) = 0.0139 * 10^{-11}$$

$$F_{T_y} = F_{4,6} + F_3 \sin 48° - (F_2 \sin 42° + F_5 \sin 48° - (F_8 \sin 48°) = 5.6717 * 10^{-11}$$

$F_T = 5.6717 * 10^{-11}$ N

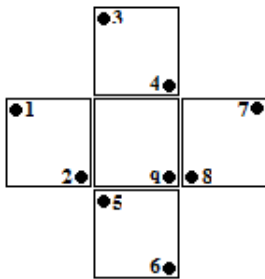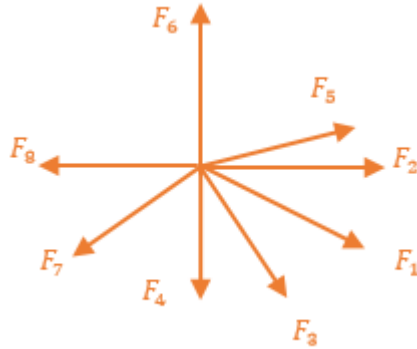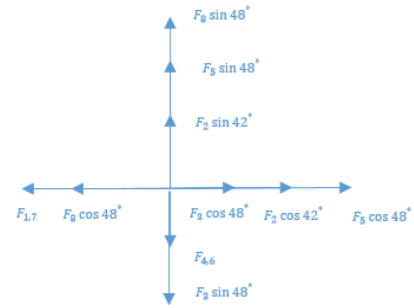**Fig.8** a.3-1)   a.3-2)   a.3-3)

$$|F_1| = |F_3| = \frac{23.04 * 10^{-29}}{1768 * 10^{-18}} = 0.0130 * 10^{-11}$$

$$|F_2| = |F_4| = |F_6| = \frac{23.04 * 10^{-29}}{400 * 10^{-18}} = 0.0576 * 10^{-11}$$

$$|F_7| = \frac{23.04 * 10^{-29}}{724 * 10^{-18}} = 0.0318 * 10^{-11}$$

$$|F_5| = \frac{23.04 * 10^{-29}}{328 * 10^{-18}} = 0.0702 * 10^{-11}$$

$$|F_8| = \frac{23.04 * 10^{-29}}{4 * 10^{-18}} = 5.76 * 10^{-11}$$

$$F_{2,8} = F_8 - F_2 = (5.76 * 10^{-11}) - (0.0130 * 10^{-11}) = 5.747 * 10^{-11}$$

$$F_{4,6} = F_4 - F_6 = 0$$

$$F_{T_x} = F_{2,8} + F_7 \cos 42^\circ - (F_5 \cos 6^\circ + F_1 \cos 25^\circ + F_3 \cos 65^\circ) = 5.6837 * 10^{-11}$$

$$F_{T_y} = F_1 \sin 25^\circ + F_3 \sin 65^\circ + F_7 \sin 42^\circ - (F_5 \sin 6^\circ) = 0.031 * 10^{-11}$$

$$\mathbf{F_T = 5.6837 * 10^{-11} \ N}$$

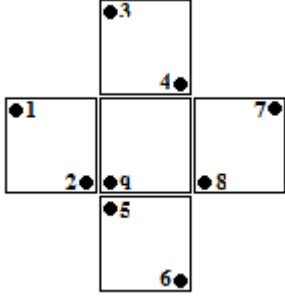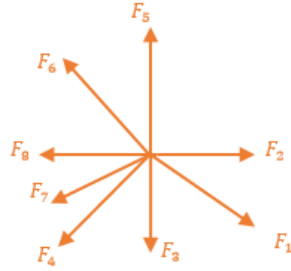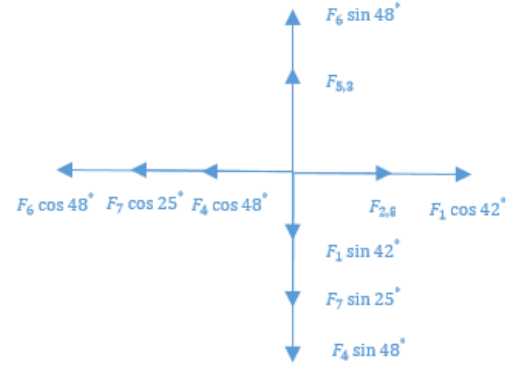**Fig.9** a.4-1)   a.4-2)   a.4-3)

$$|F_1| = |F_4| = |F_6| = \frac{23.04 * 10^{-29}}{724 * 10^{-18}} = 0.0318 * 10^{-11}$$

$$|F_2| = |F_5| = \frac{23.04 * 10^{-29}}{4 * 10^{-18}} = 5.76 * 10^{-11}$$

$$|F_3| = \frac{23.04 * 10^{-29}}{38 * 38 * 10^{-18}} = 0.0159 * 10^{-11}$$

$$|F_7| = \frac{23.04 * 10^{-29}}{1768 * 10^{-18}} = 0.0130 * 10^{-11}$$

$$|F_8| = \frac{23.04 * 10^{-29}}{400 * 10^{-18}} = 0.0576 * 10^{-11}$$

$$F_{2,8} = F_2 - F_8 = (5.76 * 10^{-11}) - (0.0576 * 10^{-11}) = 5.7024 * 10^{-11}$$

$$F_{5,3} = F_5 - F_3 = (5.76 * 10^{-11}) - (0.0159 * 10^{-11}) = 5.7441 * 10^{-11}$$

$$F_{T_x} = F_{2,8} + F_1 \cos 42° - (F_6 \cos 48° + F_7 \cos 25° + F_4 \cos 48°) = 5.6314 * 10^{-11}$$

$$F_{T_y} = F_{5,3} + F_6 \sin 48° - (F_1 \sin 42° + F_7 \sin 25° + F_4 \sin 48°) = 5.6986 * 10^{-11}$$

$$\mathbf{F_T = 8.0116 * 10^{-11} \, N}$$

$$\mathbf{F_{T_{a.9}} > F_{T_{a.8}} > F_{T_{a.7}} > F_{T_{a.6}}}$$

The reason for this difference in output is that a single electron cell is used in the voter cell. Table (3) shows the output of the proposed design.

$$M(A, \overline{B}, \overline{C}) = A\overline{B} + A\overline{C} + \overline{B}\overline{C} \tag{4}$$

Table 3 All configurations of proposed design

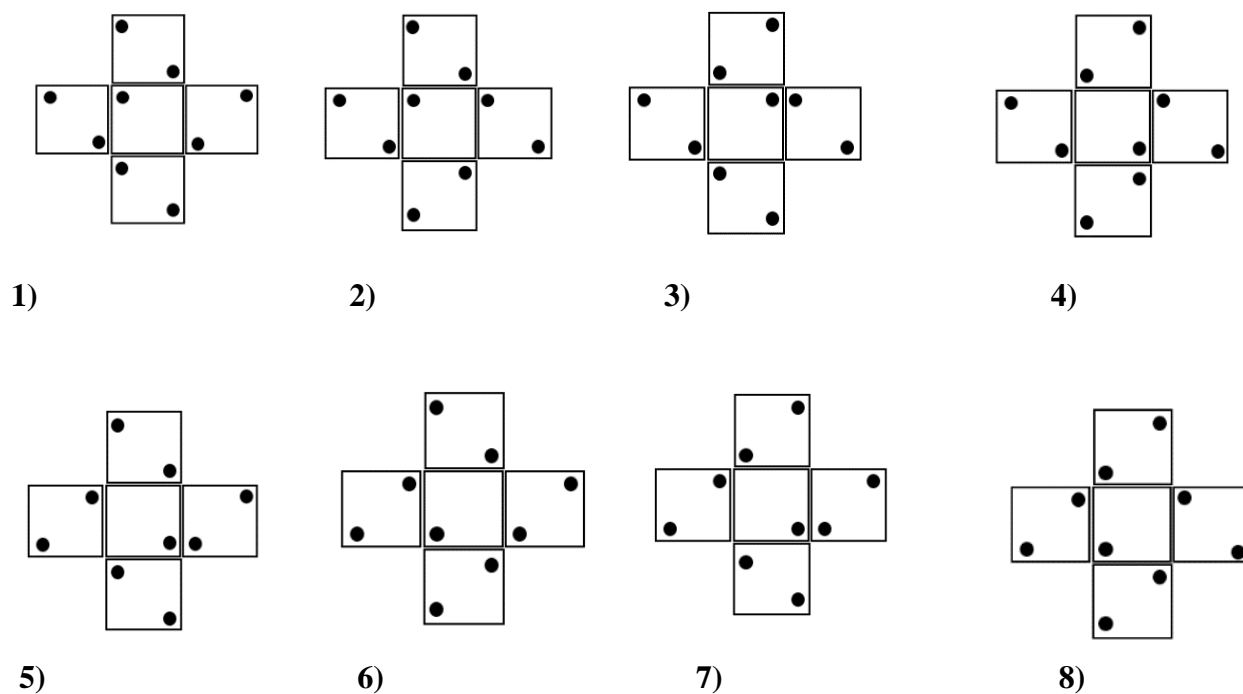| State	A	B	C_{in}	Proposed M (A,$\overline{B}$, $\overline{C_{in}}$)
1	0	0	0	1
2	0	0	1	0
3	0	1	0	0
4	0	1	1	0
5	1	0	0	1
6	1	0	1	1
7	1	1	0	1
8	1	1	1	0

1)   2)   3)   4)

5)   6)   7)   8)

Fig. 10 The proposed design in all states

A biological neuron can be used in the design of QCA circuits. Even if a biological neuron has a lot of inputs, we are using a three-input neuron with two negative weighted inputs as shown in figure 11. This neuron functions as a majority gate. Since the number of inputs with logical 1 exceeds the number of ones with logical 0, then the QCA cell with the majority function becomes 1, which is equivalent to the neuron fires when the summation of inputs reaches a threshold.
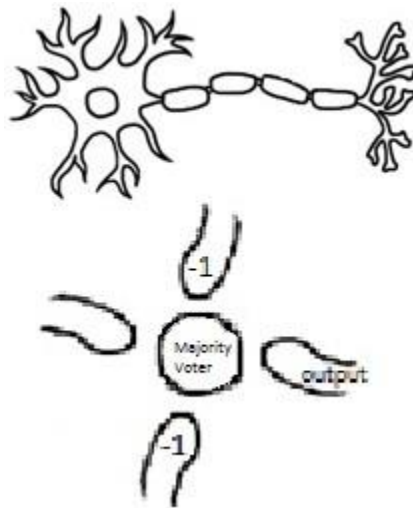

Fig. 11 Modelling Majority gate and neural network

5. Conclusion

Nearly all QCA circuits are implemented with majority and inverter gates. Designing more optimized gates can be achieved using the Bio-Inspired Models. In this article, a new three-input majority gate was proposed by omitting an electron in the voter cell, leaving four dots and only one electron, instead of two which can implement the negative weighted of two inputs out of three. By decreasing the number of electrons in the Quantum Dot Cellular Automata (QCA), the number of cells in a circuit were reduced, thus decreasing power consumption. The effectiveness of the proposed ideas was investigated by physical and mathematical proofs, and their validity ascertained through the mentioned proofs.

Conflict of interest
No competing financial interests exist.

References

1.   Wanlass, F.M., *Low stand-by power complementary field effect circuitry*. 1967, Google Patents.
2.   Moore, G.E., *Cramming more components onto integrated circuits*. 1965, McGraw-Hill New York, NY, USA:.
3.   Lent, C.S. and P.D. Tougaw, *A device architecture for computing with quantum dots.* Proceedings of the IEEE, 1997. **85**(4): p. 541-557.
4.   Lent, C.S., et al., *Quantum cellular automata.* Nanotechnology, 1993. **4**(1): p. 49.
5.   Campos, C.A.T., et al., *Use: a universal, scalable, and efficient clocking scheme for QCA.* IEEE Transactions on computer-aided design of integrated circuits and systems, 2016. **35**(3): p. 513-517.
6.   Tougaw, P.D. and C.S. Lent, *Dynamic behavior of quantum cellular automata.* Journal of Applied Physics, 1996. **80**(8): p. 4722-4736.
7.   Tougaw, P.D. and C.S. Lent, *Logical devices implemented using quantum cellular automata.* Journal of Applied physics, 1994. **75**(3): p. 1818-1825.
8.   Shin, S.-H., J.-C. Jeon, and K.-Y. Yoo. *Wire-crossing technique on quantum-dot cellular automata*. in *NGCIT2013, the 2nd international conference on next generation computer and information technology*. 2013.
9.   Orlov, A.O., et al., *Experimental demonstration of a binary wire for quantum-dot cellular automata.* Applied physics letters, 1999. **74**(19): p. 2875-2877.
10.   Esfahani, Z.N., M. Sam, and K. Navi, *Design of new NAND/NOR gates in QCA using single electron cells.* International Journal of Circuits and Architecture Design, 2016. **2**(2): p. 132-141.
11.   Taheri, M., et al., *A Novel Majority Based Imprecise 4: 2 Compressor with Respect to the Current and Future VLSI Industry.* Microprocessors and Microsystems, 2019: p. 102962.
12.   Zhang, C.N., M. Zhao, and M. Wang, *Logic operations based on single neuron rational model.* IEEE Transactions on neural networks, 2000. **11**(3): p. 739-747.
13.   Chowdhury, A., et al. *Simulations of threshold logic unit problems using memristor based synapses and CMOS neuron*. in *2017 3rd International Conference on Electrical Information and Communication Technology (EICT)*. 2017. IEEE.
14.   Adonias, G.L., et al., *Utilizing Neurons for Digital Logic Circuits: A Molecular Communications Analysis.* arXiv preprint arXiv:1909.02833, 2019.
15.   Hook IV, L.R. and S.C. Lee, *Design and simulation of 2-D 2-dot quantum-dot cellular automata logic.* IEEE Transactions on Nanotechnology, 2011. **10**(5): p. 996-1003.
16.   Ghosh, M., D. Mukhopadhyay, and P. Dutta. *A 2D 2 Dot 1 electron quantum dot cellular automata based logically reversible 2: 1 multiplexer*. in *Research in Computational Intelligence and Communication Networks (ICRCICN), 2015 IEEE International Conference on*. 2015. IEEE.

17.   Mondal, S., et al. *A Design and Application Case Study of Binary Semaphore Using 2 Dimensional 2 Dot 1 Electron Quantum Dot Cellular Automata*. in *Annual Convention of the Computer Society of India*. 2018. Springer.

18.   Farzaneh, F., R.F. Mirzaee, and K. Navi, *A novel 3D three/five-input majority-based full adder in nanomagnetic logic.* Journal of Computational Electronics, 2019. **18**(1): p. 364-373.

19.   Bhoi, B.K., et al., *An Explicit Cell-Based Nesting Robust Architecture and Analysis of Full Adder*, in *Recent Trends in Communication, Computing, and Electronics*. 2019, Springer. p. 547-555.

20.   Seyedi, S. and N.J. Navimipour, *An optimized design of full adder based on nanoscale quantum-dot cellular automata.* Optik, 2018. **158**: p. 243-256.

21.   Ghosh, M., D. Mukhopadhyay, and P. Dutta, *Design of an arithmetic circuit using non-reversible adders in 2 dot 1 electron QCA.* Microsystem Technologies, 2019. **25**(5): p. 1719-1729.

22.   Maor, E., *The Pythagorean theorem: a 4,000-year history*. 2007: Princeton University Press.

23.   Hvidsten, M., *Geometry with geometry explorer*. 2005: McGraw-Hill.